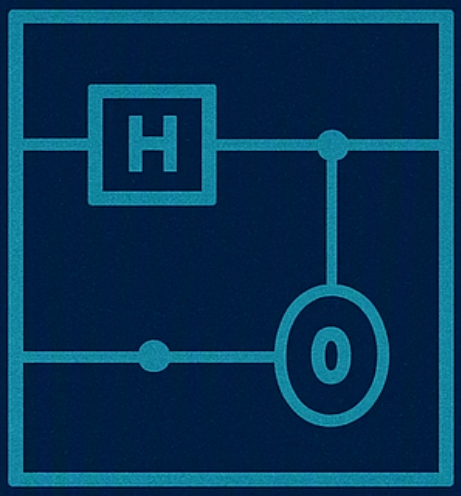
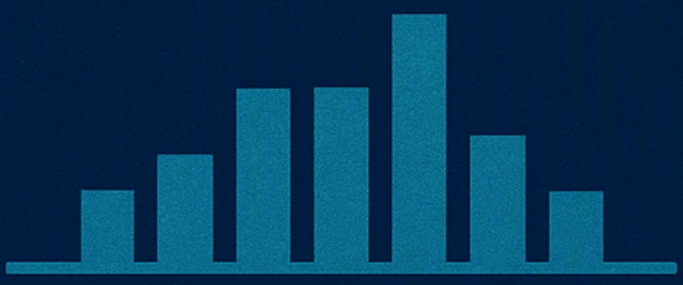
# BASIC PRINCIPLES OF QUANTUM COMPUTING









# Basic Principles of Quantum Computing

The Publicator using openai/gpt-oss-120b

# Contents

**Basic Principles of Quantum Computing** **3**
1. Introduction . . . 4
1.1 Motivation for Quantum Computing . . . 4
1.2 Potential Impact . . . 4
1.3 Scope and Organization of the Paper . . . 4
2. Fundamental Concepts . . . 6
2.1 Superposition - The Quantum Bit's Dual Nature . . . 6
2.2 Entanglement - Correlations Beyond Classical Limits . . . 6
2.3 Quantum Measurement - From Possibility to Reality . . . 6
2.4 Interplay of the Core Concepts . . . 7
3. Qubits and Quantum State Representation . . . 8
3.1 Dirac Notation and the Computational Basis . . . 8
3.2 Geometric Visualization: The Bloch Sphere . . . 8
3.3 Mixed States and Density Matrices . . . 8
3.4 Summary of Representations . . . 9
4. Quantum Gates and Operations . . . 10
4.1 Single-Qubit Gates: The Pauli Set and the Hadamard/Phase Family . . . 10
4.2 Two-Qubit Entangling Gates . . . 10
4.3 Universality: Building Any Unitary from a Finite Set . . . 10
4.4 Gate Composition and State Evolution . . . 11
4.5 Practical Considerations for Gate Implementation . . . 11
5. Quantum Circuits . . . 12
5.1 Circuit Model Construction . . . 12
5.2 Gate Sequencing and Composition . . . 12
5.3 Circuit Depth and Width . . . 12
5.4 Design Considerations for Algorithm Construction . . . 13
5.5 Illustrative Example: A Simple Entanglement Circuit . . . 13
5.6 Summary . . . 13
6. Key Quantum Algorithms . . . 14
6.1 Deutsch-Jozsa Algorithm . . . 14
6.2 Grover's Unstructured Search . . . 14
6.3 Shor's Factoring Algorithm . . . 14
6.4 Comparative Perspective on Algorithmic Advantage . . . 15
7. Quantum Error Correction and Fault Tolerance . . . 17
7.1 Sources of Decoherence and Noise . . . 17
7.2 Standard Error Models . . . 17
7.3 The Quantum Error-Correction Paradigm . . . 17
7.4 Concatenated Codes . . . 17
7.5 Topological Surface Codes . . . 18
7.6 Fault-Tolerance Thresholds . . . 18
7.7 Fault-Tolerant Logical Operations . . . 19
7.8 Summary and Outlook . . . 19
8. Physical Implementations . . . 20
8.1 Superconducting Circuits . . . 20
8.2 Trapped-Ion Qubits . . . 20
8.3 Photonic Quantum Processors . . . 20
8.4 Topological (Majorana-Based) Qubits . . . 21
8.5 Comparative Summary . . . 21

9. Challenges and Future Directions . . . . . 23
9.1 Technical Challenges . . . . . 23
9.2 Theoretical Challenges . . . . . 23
9.3 Scalability Issues . . . . . 23
9.4 Emerging Research Avenues . . . . . 24
9.5 Outlook and Recommendations . . . . . 24
10. Conclusion . . . . . 25
10.1 Recap of the Core Principles . . . . . 25
10.2 Interdependence of the Principles . . . . . 25
10.3 Outlook for Practical Quantum Computing . . . . . 25
10.4 Concluding Perspective . . . . . 26

# Basic Principles of Quantum Computing

**Abstract:** This paper presents a comprehensive overview of the foundational principles underlying quantum computing. Beginning with an introduction that motivates the field's significance and delineates its scope, we establish the physical basis for quantum information processing by detailing the core concepts of superposition, entanglement, and measurement. The mathematical formalism of qubits is then examined through Dirac notation, Bloch-sphere visualization, and density-matrix representation, providing the essential language for describing quantum states. Building on this foundation, we describe the universal set of quantum gates - including Pauli, Hadamard, Phase, and CNOT - and their matrix formulations, illustrating how these operations manipulate qubit states. The circuit model is introduced, emphasizing gate sequencing, circuit depth, and width as critical parameters for algorithm design. We subsequently review seminal quantum algorithms - Deutsch-Jozsa, Grover's search, and Shor's factoring - highlighting their provable speedups over classical approaches. Recognizing the fragility of quantum information, the discussion turns to decoherence, error models, and the development of quantum error-correcting codes such as Shor, Steane, and surface codes, together with fault-tolerance thresholds. An overview of leading physical implementations - superconducting circuits, trapped ions, photonic systems, and topological qubits - summarizes current hardware capabilities and performance metrics. Finally, we analyze outstanding technical and theoretical challenges, scalability constraints, and emerging research directions, including quantum networking and hybrid quantum-classical architectures. The conclusion synthesizes these principles, underscoring their interdependence and projecting a roadmap toward practical, large-scale quantum computation.

# 1. Introduction

## 1.1 Motivation for Quantum Computing

The exponential growth of data, the emergence of cryptographic protocols based on hard mathematical problems, and the limits of Moore's law have converged to create a pressing demand for computational paradigms that transcend classical capabilities. Classical algorithms, even when optimized, encounter insurmountable barriers for certain tasks such as factoring large integers, simulating many-body quantum systems, or searching unsorted databases. These challenges are not merely academic; they impact fields ranging from cybersecurity and materials science to drug discovery and artificial intelligence. Quantum computing offers a fundamentally different approach by exploiting quantum mechanical phenomena - most notably superposition and entanglement - to process information in ways that can provide polynomial or exponential speed-ups over the best known classical methods.

## 1.2 Potential Impact

If realized at scale, quantum computers could transform several domains:

- **Cryptography:** Shor's algorithm (see *Section 6. Key Quantum Algorithms*) can factor integers in polynomial time, threatening RSA and elliptic-curve schemes that underpin modern secure communications.
- **Materials and Chemistry:** Quantum simulation of molecular Hamiltonians promises accurate predictions of chemical properties, accelerating the design of catalysts, pharmaceuticals, and novel materials.
- **Optimization and Machine Learning:** Quantum-enhanced heuristics (e.g., quantum approximate optimization) may solve combinatorial problems and train models more efficiently than classical counterparts.
- **Fundamental Science:** By providing a testbed for quantum phenomena, quantum computers enable experimental investigations of quantum many-body physics, quantum gravity analogues, and beyond.

These prospective benefits justify substantial investment from academia, industry, and governments worldwide, as reflected in the rapid growth of quantum research programs and the emergence of a nascent quantum technology ecosystem.

## 1.3 Scope and Organization of the Paper

This paper presents a self-contained overview of the essential principles underlying quantum computing, targeting readers with a background in classical computer science or physics who seek a concise yet rigorous introduction. The exposition proceeds as follows:

1. **Fundamental Concepts** (*Section 2*) introduces the physical basis of quantum information processing, covering superposition, entanglement, and measurement.
2. **Qubits and Quantum State Representation** (*Section 3*) formalizes the mathematical description of quantum bits using Dirac notation, the Bloch sphere, and density matrices.
3. **Quantum Gates and Operations** (*Section 4*) details the universal gate set and their matrix representations, establishing how quantum states are manipulated.
4. **Quantum Circuits** (*Section 5*) explains the circuit model, gate sequencing, and the relevance of circuit depth and width for algorithm design.
5. **Key Quantum Algorithms** (*Section 6*) surveys landmark algorithms that demonstrate quantum advantage, including Deutsch-Jozsa, Grover's search, and Shor's factoring.
6. **Quantum Error Correction and Fault Tolerance** (*Section 7*) addresses decoherence, error models, and the construction of error-correcting codes that enable reliable computation.
7. **Physical Implementations** (*Section 8*) reviews the leading hardware platforms - superconducting circuits, trapped ions, photonic systems, and topological qubits - along with their current performance metrics.

8. **Challenges and Future Directions** (*Section 9*) analyzes open technical and theoretical hurdles, scalability concerns, and emerging research avenues such as quantum networking and hybrid quantum-classical architectures.

9. **Conclusion** (*Section 10*) recaps the core principles, emphasizes their interdependence, and outlines the outlook for practical quantum computing.

By systematically building from the quantum mechanical foundations to algorithmic applications and hardware realizations, the paper aims to equip the reader with a coherent mental model of how quantum computers operate, why they matter, and what obstacles remain on the path to widespread utility.

# 2. Fundamental Concepts

## 2.1 Superposition - The Quantum Bit's Dual Nature

A quantum bit, or **qubit**, differs fundamentally from a classical bit because it can exist in a *linear combination* of its basis states $|0\rangle$ and $|1\rangle$. Mathematically, a pure qubit state is written

$$|\psi\rangle = \alpha|0\rangle + \beta|1\rangle, \qquad \alpha, \beta \in \mathbb{C},\ |\alpha|^2 + |\beta|^2 = 1.$$

The coefficients $\alpha$ and $\beta$ are called **amplitudes**; their squared magnitudes give the probabilities of obtaining $|0\rangle$ or $|1\rangle$ upon measurement. This *superposition* enables a single qubit to encode more information than a classical bit, a property that becomes exponentially powerful when many qubits are combined (see Section 3 for the formal state-vector and density-matrix representations).

Key physical insights:

- **Interference** - Relative phases between amplitudes can cause constructive or destructive interference when the state evolves under quantum gates (Section 4).
- **Continuum of states** - Unlike a classical bit that is either 0 or 1, a qubit can be prepared anywhere on the surface of the Bloch sphere, providing a geometric intuition for superposition (Section 3).

## 2.2 Entanglement - Correlations Beyond Classical Limits

When two or more qubits interact, their joint state may become **entangled**, meaning it cannot be expressed as a simple product of individual qubit states. An archetypal two-qubit entangled state is the Bell state

$$|\Phi^+\rangle = \tfrac{1}{\sqrt{2}}(|00\rangle + |11\rangle).$$

In this state, measurement outcomes of the two qubits are perfectly correlated regardless of the spatial separation between them - a phenomenon with no classical analogue. Entanglement is the resource that underpins many quantum-information protocols:

- **Quantum teleportation** - transfers an unknown qubit state using a shared entangled pair and classical communication.
- **Super-dense coding** - sends two classical bits by transmitting a single qubit that is part of an entangled pair.
- **Algorithmic speed-up** - algorithms such as Shor's and Grover's (Section 6) exploit multi-qubit entanglement to explore a vast computational space simultaneously.

Entanglement can be quantified by measures such as the **von Neumann entropy** of reduced density matrices (see Section 3 for density-matrix formalism). The creation of entanglement typically requires two-qubit gates, most notably the **CNOT** gate introduced in Section 4.

## 2.3 Quantum Measurement - From Possibility to Reality

Measurement collapses a superposed quantum state onto one of the eigenstates of the observable being measured. For a single qubit measured in the computational basis $\{|0\rangle, |1\rangle\}$, the Born rule gives

$$P(0) = |\alpha|^2, \qquad P(1) = |\beta|^2,$$

and after the measurement the qubit is left in the observed eigenstate. Several important aspects follow:

- **Irreversibility** - Once a projective measurement is performed, the original superposition is lost; subsequent operations act on the post-measurement eigenstate.
- **Basis dependence** - Measuring in a different basis (e.g., the Hadamard basis $\{|+\rangle, |-\rangle\}$) yields probabilities determined by the amplitudes expressed in that basis. Changing measurement bases is a routine step in quantum algorithms (Section 6) and error-correction protocols (Section 7).
- **Partial measurement and weak measurement** - Modern experimental platforms can perform non-projective or weak measurements that only partially collapse the state, enabling feedback and adaptive control strategies.

Measurement also serves as the interface between the quantum processor and classical post-processing. The statistical outcomes of many repeated runs (shots) are used to estimate expectation values, a practice that will be revisited when discussing algorithmic results in Section 6.

## 2.4 Interplay of the Core Concepts

The three pillars - **superposition**, **entanglement**, and **measurement** - are tightly interwoven:

| Concept | Role in Quantum Information | Connection to Other Sections |
|---|---|---|
| Superposition | Provides the exponential state space; enables interference. | Formalized in Section 3 (state representation) and manipulated by gates in Section 4. |
| Entanglement | Generates non-classical correlations essential for speed-up and communication protocols. | Created by two-qubit gates (Section 4) and quantified using density matrices (Section 3). |
| Measurement | Extracts classical information; defines algorithmic output and error-syndrome detection. | Basis changes implemented by gates (Section 4); measurement outcomes feed error-correction routines (Section 7). |

Understanding these concepts establishes the physical foundation upon which the remainder of the paper builds: the precise mathematical description of qubits (Section 3), the toolbox of quantum gates (Section 4), the construction of circuits (Section 5), and ultimately the design of powerful algorithms (Section 6).

*In summary, superposition endows each qubit with a continuum of possibilities, entanglement weaves multiple qubits into inseparable wholes, and measurement translates quantum potential into classical results. Mastery of these ideas is indispensable for any further exploration of quantum computing.*

# 3. Qubits and Quantum State Representation

## 3.1 Dirac Notation and the Computational Basis

A single qubit is a two-level quantum system. Its state vector lives in a two-dimensional Hilbert space $\mathcal{H} \cong \mathbb{C}^2$ and is most compactly expressed with **Dirac (bra-ket) notation**:

$|\psi\rangle = \alpha|0\rangle + \beta|1\rangle, \qquad \alpha, \beta \in \mathbb{C},\ |\alpha|^2 + |\beta|^2 = 1.$

The kets $|0\rangle$ and $|1\rangle$ form the **computational basis**, which coincides with the eigenstates of the Pauli -$Z$ operator:

$Z|0\rangle = +|0\rangle, \qquad Z|1\rangle = -|1\rangle.$

The corresponding bras are the Hermitian conjugates, $\langle 0| = (|0\rangle)^\dagger$ and $\langle 1| = (|1\rangle)^\dagger$. Inner products give the overlap between states, e.g. $\langle 0|\psi\rangle = \alpha$. The **outer product** $|\psi\rangle\langle\phi|$ is a $2 \times 2$ operator that will be useful when we introduce density matrices (Section 3.3).

## 3.2 Geometric Visualization: The Bloch Sphere

Because the global phase of a qubit state is physically irrelevant, any pure state can be mapped to a point on the surface of a unit sphere - the **Bloch sphere**. By parametrising the amplitudes as

$\alpha = \cos\!\left(\tfrac{\theta}{2}\right), \qquad \beta = e^{i\phi}\sin\!\left(\tfrac{\theta}{2}\right), \qquad 0 \le \theta \le \pi,\ 0 \le \phi < 2\pi,$

the state becomes

$|\psi\rangle = \cos\!\left(\tfrac{\theta}{2}\right)|0\rangle + e^{i\phi}\sin\!\left(\tfrac{\theta}{2}\right)|1\rangle.$

The pair $(\theta, \phi)$ are the spherical coordinates of a vector

$\mathbf{r} = (\sin\theta\cos\phi,\ \sin\theta\sin\phi,\ \cos\theta)$

that points from the origin to the surface of the sphere. The north pole $(0, 0, 1)$ corresponds to $|0\rangle$, the south pole $(0, 0, -1)$ to $|1\rangle$, while points on the equator represent equal-amplitude superpositions with varying relative phase (e.g., $|+\rangle = (|0\rangle + |1\rangle)/\sqrt{2}$ at $\phi = 0$).

The Bloch sphere provides an intuitive picture of **single-qubit operations**: any unitary $U \in \mathrm{SU}(2)$ acts as a rotation of $\mathbf{r}$ about some axis. This geometric view will be repeatedly invoked when discussing gate implementations in Section 4.

## 3.3 Mixed States and Density Matrices

In realistic settings a qubit may be **partially decohered** or entangled with an environment, so its description must go beyond a single ket. The **density operator** (or density matrix) $\rho$ captures both pure and mixed states:

$\rho = \sum_k p_k\,|\psi_k\rangle\langle\psi_k|, \qquad p_k \ge 0,\ \sum_k p_k = 1.$

- For a pure state $|\psi\rangle$ the ensemble reduces to a single term, yielding $\rho = |\psi\rangle\langle\psi|$ and $\mathrm{Tr}(\rho^2) = 1$.
- For a mixed state $\mathrm{Tr}(\rho^2) < 1$; the degree of mixedness quantifies the loss of coherence.

In the computational basis the density matrix takes the explicit form

$\rho = \begin{pmatrix} \rho_{00} & \rho_{01} \\ \rho_{10} & \rho_{11} \end{pmatrix}, \qquad \rho_{ij} = \langle i|\rho|j\rangle,$

with the constraints $\rho = \rho^\dagger$ (Hermiticity) and $\mathrm{Tr}\,\rho = 1$ (unit trace). The Bloch-sphere representation extends to mixed states by allowing the Bloch vector $\mathbf{r}$ to lie **inside** the unit sphere:

$\rho = \tfrac{1}{2}(\mathbb{I} + \mathbf{r}\cdot\sigma), \qquad \|\mathbf{r}\| \le 1,$

where $\sigma = (X, Y, Z)$ are the Pauli matrices. Pure states sit on the surface ($\|\mathbf{r}\| = 1$), while the completely mixed state $\rho = \mathbb{I}/2$ sits at the origin ($\mathbf{r} = 0$).

Density matrices are indispensable for:

- **Describing decoherence** (Section 7) - e.g., amplitude-damping and phase-damping channels act as completely positive trace-preserving (CPTP) maps on $\rho$.

- **Analyzing entanglement** - reduced density matrices obtained by tracing out subsystems reveal whether a multi-qubit state is entangled (see Section 2).

- **Predicting measurement statistics** - the probability of obtaining outcome $i$ when measuring in basis $\{|i\rangle\}$ is $p(i) = \langle i|\rho|i\rangle = \mathrm{Tr}(\rho|i\rangle\langle i|)$.

## 3.4 Summary of Representations

| Representation | Formalism | Visual Aid | When to Use |
|---|---|---|---|
| **Dirac ket** | $\|\psi\rangle = \alpha\|0\rangle + \beta\|1\rangle$ | - | Pure state, analytical calculations, gate algebra (Section 4). |
| **Bloch sphere** | $\mathbf{r} = (\sin\theta\cos\phi, \sin\theta\sin\phi, \cos\theta)$ | 3-D sphere (surface for pure, interior for mixed) | Intuition about single-qubit rotations, error visualization. |
| **Density matrix** | $\rho = \sum_k p_k \|\psi_k\rangle\langle\psi_k\|$ | Bloch vector inside sphere | Mixed states, decoherence modelling, entanglement analysis. |

These three complementary viewpoints form the backbone of quantum-state bookkeeping throughout the remainder of the paper. They enable us to move seamlessly from the abstract linear-algebraic description (Section 4) to concrete circuit implementations (Section 5) and to the algorithmic exploits of quantum superposition and entanglement (Section 6).

# 4. Quantum Gates and Operations

## 4.1 Single-Qubit Gates: The Pauli Set and the Hadamard/Phase Family

Single-qubit gates are unitary operators $U \in \mathbb{C}^{2\times 2}$ that rotate the Bloch vector of a qubit (see **Section 3** for the Bloch-sphere representation). The most frequently used single-qubit gates form a *universal* generating set:

| Gate | Symbol | Matrix (computational basis $\{\|0\rangle, \|1\rangle\}$) | Action on $\|\psi\rangle = \alpha\|0\rangle + \beta\|1\rangle$ |
|---|---|---|---|
| **Pauli-X** (bit-flip) | $X$ | $X = \begin{pmatrix} 0 & 1 \\ 1 & 0 \end{pmatrix}$ | Swaps amplitudes: $\alpha\|0\rangle + \beta\|1\rangle \xrightarrow{X} \beta\|0\rangle + \alpha\|1\rangle$ |
| **Pauli-Y** (bit- and phase-flip) | $Y$ | $Y = \begin{pmatrix} 0 & -i \\ i & 0 \end{pmatrix}$ | Introduces a relative phase of $\pm i$ while swapping amplitudes. |
| **Pauli-Z** (phase-flip) | $Z$ | $Z = \begin{pmatrix} 1 & 0 \\ 0 & -1 \end{pmatrix}$ | Leaves $\|0\rangle$ unchanged, flips the sign of $\|1\rangle$: $\alpha\|0\rangle + \beta\|1\rangle \xrightarrow{Z} \alpha\|0\rangle - \beta\|1\rangle$. |
| **Hadamard** | $H$ | $H = \frac{1}{\sqrt{2}} \begin{pmatrix} 1 & 1 \\ 1 & -1 \end{pmatrix}$ | Creates an equal superposition: $\|0\rangle \to \frac{\|0\rangle+\|1\rangle}{\sqrt{2}}$, $\|1\rangle \to \frac{\|0\rangle-\|1\rangle}{\sqrt{2}}$. This gate implements the basis change required for many measurement strategies (cf. **Section 2**). |
| **Phase (S)** | $S$ | $S = \begin{pmatrix} 1 & 0 \\ 0 & i \end{pmatrix}$ | Adds a $\pi/2$ phase to $\|1\rangle$: $\alpha\|0\rangle + \beta\|1\rangle \xrightarrow{S} \alpha\|0\rangle + i\beta\|1\rangle$. |
| * **$\pi/8$ (T)** | $T$ | $T = \begin{pmatrix} 1 & 0 \\ 0 & e^{i\pi/4} \end{pmatrix}$ | Adds a $\pi/4$ phase to $\|1\rangle$; together with $S$ it generates arbitrary single-qubit rotations. |

All of the above are **unitary** ($U^\dagger U = I$) and therefore preserve the norm of the state vector, a requirement highlighted in **Section 3**'s discussion of density-matrix purity.

## 4.2 Two-Qubit Entangling Gates

Entanglement, introduced in **Section 2**, cannot be generated by single-qubit operations alone. The canonical two-qubit gate is the **Controlled-NOT (CNOT)**:

$$\mathrm{CNOT} = \begin{pmatrix} 1 & 0 & 0 & 0 \\ 0 & 1 & 0 & 0 \\ 0 & 0 & 0 & 1 \\ 0 & 0 & 1 & 0 \end{pmatrix}, \qquad |c\rangle|t\rangle \xrightarrow{\mathrm{CNOT}} |c\rangle|t \oplus c\rangle.$$

The first qubit (control) determines whether the second qubit (target) is flipped. Acting on a separable input such as $\frac{|0\rangle+|1\rangle}{\sqrt{2}} \otimes |0\rangle$ yields the Bell state $\frac{|00\rangle+|11\rangle}{\sqrt{2}}$, a maximally entangled resource used throughout **Section 6**.

Other useful entangling gates include:

| Gate | Symbol | Matrix (ordered as $\|00\rangle, \|01\rangle, \|10\rangle, \|11\rangle$) | Typical Use |
|---|---|---|---|
| **Controlled-Z (CZ)** | $CZ$ | $CZ = \mathrm{diag}(1, 1, 1, -1)$ | Phase-based entanglement; often easier to implement in superconducting circuits (see **Section 8**). |
| **iSWAP** | $i$SWAP | $i\mathrm{SWAP} = \begin{pmatrix} 1 & 0 & 0 & 0 \\ 0 & 0 & i & 0 \\ 0 & i & 0 & 0 \\ 0 & 0 & 0 & 1 \end{pmatrix}$ | Swaps amplitudes of $\|01\rangle$ and $\|10\rangle$ with a $\pi/2$ phase; natural in certain ion-trap couplings. |

All two-qubit gates are also unitary and act on the **tensor product** space $\mathbb{C}^2 \otimes \mathbb{C}^2$, consistent with the density-matrix formalism of **Section 3**.

## 4.3 Universality: Building Any Unitary from a Finite Set

A *universal* gate set is a finite collection of gates from which any $n$-qubit unitary $U \in \mathbb{C}^{2^n \times 2^n}$ can be approximated to arbitrary precision. The following theorem (often called the **Solovay-Kitaev theorem**) underpins the choice of gates in this section:

> **Theorem (Solovay-Kitaev).**
> If a finite gate set generates a dense subgroup of $SU(2)$ (or $SU(2^n)$ when combined with an entangling two-qubit gate), then any target unitary can be approximated with polylogarithmic overhead in the desired precision $\epsilon$.

Consequently, the set
$\{H, S, T, \text{CNOT}\}$ is universal:

- The single-qubit subgroup $\langle H, S, T\rangle$ densely covers $SU(2)$ (any rotation on the Bloch sphere).
- Adding **CNOT** supplies the necessary entangling power to reach the full $SU(2^n)$ for arbitrary $n$.

Alternative universal families (e.g., $\{X, Z, \text{CNOT}\}$ together with arbitrary single-qubit rotations) are mathematically equivalent; the choice in practice depends on hardware constraints discussed in **Section 8**.

## 4.4 Gate Composition and State Evolution

When a sequence of gates $\{U_k\}$ is applied to an initial state $|\psi_0\rangle$, the final state is obtained by left-multiplication in reverse order:

$|\psi_{\text{out}}\rangle = U_m \cdots U_2 U_1 |\psi_0\rangle$.

Because each gate is unitary, the overall transformation remains unitary, preserving the trace and positivity of the density matrix $\rho = |\psi\rangle\langle\psi|$ (see **Section 3**). This property enables **circuit-level reasoning** (the focus of **Section 5**) and guarantees that probabilities derived via the Born rule stay normalized.

*Example:*
Starting from $|0\rangle$, apply $H$ then $S$ then $X$:

$$|0\rangle \xrightarrow{H} \frac{|0\rangle + |1\rangle}{\sqrt{2}} \xrightarrow{S} \frac{|0\rangle + i|1\rangle}{\sqrt{2}} \xrightarrow{X} \frac{i|0\rangle + |1\rangle}{\sqrt{2}}.$$

The overall matrix product is $XSH = \frac{1}{\sqrt{2}} \begin{pmatrix} i & 1 \\ 1 & i \end{pmatrix}$, a valid single-qubit unitary.

## 4.5 Practical Considerations for Gate Implementation

While the abstract matrices capture the ideal logical action, real hardware introduces **control errors**, **decoherence**, and **crosstalk**. The error models introduced in **Section 7** (e.g., depolarizing and dephasing channels) are applied to each gate as a quantum operation $\mathcal{E}_U(\rho) = (1-p)U\rho U^\dagger + p\,\mathcal{N}(\rho)$, where $p$ is the gate error probability and $\mathcal{N}$ denotes the noise map.

Key practical points:

- **Gate fidelity** is typically quoted as the average gate fidelity $F_{\text{avg}} = \int \langle\psi|U^\dagger \mathcal{E}_U(|\psi\rangle\langle\psi|)U|\psi\rangle d\psi$. Values above 99.9 % are now routine for single-qubit gates on superconducting and trapped-ion platforms (see **Section 8**).
- **Gate time** matters because decoherence scales with the duration of the operation; fast single-qubit rotations (tens of nanoseconds) are much shorter than two-qubit entangling gates (hundreds of nanoseconds to microseconds).
- **Connectivity constraints** (e.g., linear nearest-neighbor coupling) often require additional SWAP gates, which are themselves decomposed into three CNOTs. This overhead directly influences circuit depth, a topic explored in **Section 5**.

Understanding these nuances is essential for translating the abstract gate set presented here into **fault-tolerant** quantum circuits later in the paper.

# 5. Quantum Circuits

## 5.1 Circuit Model Construction

The circuit model treats a quantum computation as a sequence of unitary operations (gates) acting on an initial register of qubits, followed by a measurement stage that extracts classical outcomes. The model is the quantum analogue of classical Boolean circuits and is the foundation for all algorithmic discussions in **Section 6**.

- **Qubit Register** - A set of $n$ qubits prepared in a known state, typically $|0\rangle^{\otimes n}$. Using the Dirac notation introduced in **Section 3**, the register is represented as a column vector in a $2^n$-dimensional Hilbert space.

- **Gate Layering** - Each gate corresponds to a unitary matrix (see **Section 4**). A layer consists of gates that act on disjoint subsets of qubits and therefore can be applied simultaneously. The overall unitary of the circuit is the ordered product of the layer unitaries, applied from right-most (first) to left-most (last).

- **Measurement Block** - After the final gate layer, projective measurements are performed in a chosen basis (commonly the computational basis). The measurement collapses the state according to the Born rule, linking the quantum process back to the classical world as described in **Section 2**.

The circuit diagram is a compact visual language: horizontal lines denote qubit wires, boxes denote single-qubit gates, and symbols such as the  -control denote two-qubit entangling gates (e.g., CNOT). This graphical notation makes the sequencing of operations explicit and aids reasoning about resource requirements.

## 5.2 Gate Sequencing and Composition

A quantum algorithm is realized by **sequencing** gates in a way that steers the initial state toward a target superposition or entangled state. The composition rules are:

1. **Matrix Multiplication Order** - If a circuit applies gates $U_1, U_2, \ldots, U_k$ in that temporal order, the overall unitary is
   $U_{\text{total}} = U_k\, U_{k-1}\, \ldots\, U_1$.
   This convention matches the left-multiplication rule highlighted in **Section 4**.
2. **Tensor Product for Parallel Gates** - Gates acting on different qubits within the same layer are combined via the tensor product:
   $U_{\text{layer}} = U_a \otimes U_b \otimes \cdots$.
3. **Entangling Operations** - Two-qubit gates such as CNOT generate the entanglement discussed in **Section 2**. By interleaving single-qubit rotations (Hadamard, Phase, etc.) with CNOTs, one can create arbitrary multi-qubit unitaries, a fact guaranteed by the universality of the gate set described in **Section 4**.
4. **Ancilla Management** - Additional qubits (ancillae) may be introduced to facilitate reversible computation or to store intermediate results. Proper uncomputation (reversing the ancilla's evolution) is essential to avoid residual entanglement that would corrupt the final measurement.

## 5.3 Circuit Depth and Width

Two primary resource metrics govern the feasibility of a quantum circuit:

| Metric | Definition | Algorithmic Impact |
|---|---|---|
| **Depth** | The number of sequential gate layers (i.e., the longest path from input to output when parallelism is maximized). | Determines the total execution time on a given hardware platform. Greater depth increases exposure to decoherence and gate errors, linking directly to the error models of **Section 7**. |
| **Width** | The number of qubits (wires) required, including ancillae. | Influences the physical qubit count and connectivity demands. Wide circuits may exceed the qubit budget of near-term devices, prompting algorithmic redesigns (e.g., space-time trade-offs). |

**Depth-Width Trade-off** - Many algorithms can be re-expressed to reduce depth at the cost of additional ancilla qubits, or vice-versa. For instance, the quantum Fourier transform can be implemented with $O(n^2)$ depth using only $n$ qubits, or with $O(\log n)$ depth by employing $O(n \log n)$ ancillae and parallel controlled-phase gates. Such trade-offs are central to the design considerations highlighted in **Section 6**.

## 5.4 Design Considerations for Algorithm Construction

When translating an algorithmic description into a concrete circuit, the following factors guide the engineer:

1. **Connectivity Constraints** - Real hardware often permits only nearest-neighbor two-qubit interactions. To respect this topology, SWAP gates are inserted, which increase depth. The impact of added SWAPs is quantified in **Section 7**, where error accumulation is modeled.
2. **Gate Fidelity vs. Depth** - High-fidelity single-qubit gates can be executed quickly, whereas two-qubit gates typically have lower fidelity and longer duration. Minimizing the number of entangling layers (depth) can therefore improve overall success probability.
3. **Parallelism Opportunities** - By grouping commuting gates into the same layer, one reduces depth without increasing width. Commutativity can be identified using the algebraic properties of the Pauli group (Section 4).
4. **Ancilla Reuse** - After an ancilla has been measured or uncomputed, it can be recycled for later subroutines, effectively reducing width. Care must be taken to ensure that residual entanglement is fully removed, as discussed in the measurement formalism of **Section 2**.
5. **Algorithm-Specific Patterns** - Certain algorithms exhibit characteristic circuit motifs (e.g., the "oracle" block in Grover's search, the modular exponentiation block in Shor's algorithm). Recognizing these patterns enables modular circuit design and reuse of optimized sub-circuits.

## 5.5 Illustrative Example: A Simple Entanglement Circuit

Consider a two-qubit circuit that creates a Bell state, a fundamental resource for many algorithms in **Section 6**.

1. **Initialize** the register in $|00\rangle$.
2. **Apply** a Hadamard gate $H$ to qubit 0 (single-qubit rotation on the Bloch sphere, Section 3).
3. **Apply** a CNOT gate with qubit 0 as control and qubit 1 as target (entangling gate, Section 4).

The circuit depth is 2 (one single-qubit layer, one two-qubit layer) and the width is 2. The resulting state is $|\Phi^+\rangle = \frac{1}{\sqrt{2}}(|00\rangle + |11\rangle)$,
which exhibits maximal entanglement as defined in **Section 2**. This minimal example demonstrates how gate sequencing, depth, and width interplay to produce a non-classical resource.

## 5.6 Summary

The circuit model provides a concrete, hardware-agnostic language for expressing quantum computations. By carefully arranging gates into parallel layers, managing ancilla qubits, and balancing depth against width, designers can craft circuits that respect the physical limits highlighted in **Section 7** while exploiting the superposition and entanglement resources described in **Section 2**. These principles set the stage for the algorithmic constructions explored in **Section 6** and the subsequent discussions on error mitigation, implementation, and scalability.

# 6. Key Quantum Algorithms

## 6.1 Deutsch-Jozsa Algorithm

The Deutsch-Jozsa problem asks whether a black-box function $f : \{0,1\}^n \to \{0,1\}$ is **constant** (same output for all inputs) or **balanced** (outputs 0 for exactly half of the inputs and 1 for the other half).
Classically, in the worst case one must evaluate $f$ on $2^{n-1}+1$ inputs to be certain of the answer.

The quantum solution proceeds as follows (see **Section 5** for the circuit model):

1. **State preparation** - Initialise an $n$-qubit register in $|0\rangle^{\otimes n}$ and an ancilla qubit in $|1\rangle$.

2. **Hadamard layer** - Apply a Hadamard gate (Section 4) to every qubit, creating a uniform superposition $\frac{1}{\sqrt{2^n}}\sum_x |x\rangle$ and flipping the ancilla to $\frac{|0\rangle-|1\rangle}{\sqrt{2}}$.

3. **Oracle query** - Implement the unitary $U_f$ that maps $|x\rangle|y\rangle \to |x\rangle|y \oplus f(x)\rangle$. Because the ancilla is in a phase-kickback state, the oracle imprints a global phase $(-1)^{f(x)}$ on each basis component.

4. **Second Hadamard layer** - Apply Hadamards again to the first $n$ qubits.

If $f$ is constant, constructive interference drives the final state to $|0\rangle^{\otimes n}$; if $f$ is balanced, destructive interference yields a state orthogonal to $|0\rangle^{\otimes n}$. A single measurement of the first register therefore distinguishes the two cases with **certainty after one oracle call**.

**Algorithmic advantage** - The quantum query complexity is 1 versus the classical $\Theta(2^{n-1})$. The speed-up stems directly from **superposition** (Section 2) and **interference** of amplitudes (Section 3), illustrating how quantum parallelism can collapse an exponential search space into a single measurement outcome.

## 6.2 Grover's Unstructured Search

Given an unsorted database of $N = 2^n$ items and a predicate $f$ that marks a unique "target" item ($f(x) = 1$ iff $x$ is the solution), the classical worst-case cost is $O(N)$ evaluations.

Grover's algorithm achieves a quadratic speed-up using the following building blocks (see **Section 5** for the circuit layout):

1. **Uniform superposition** - A Hadamard layer on $n$ qubits creates $\frac{1}{\sqrt{N}}\sum_x |x\rangle$.

2. **Oracle phase flip** - The unitary $U_f$ applies a $-1$ phase to the marked state, leaving all others unchanged.

3. **Diffusion (inversion-about-the-mean) operator** - Implemented with Hadamards, a phase-flip on $|0\rangle^{\otimes n}$, and another Hadamard layer, this step reflects the state vector about the average amplitude.

Repeating the **Grover iterate** (oracle + diffusion) $\approx \frac{\pi}{4}\sqrt{N}$ times amplifies the amplitude of the target state to near-unity. A final measurement yields the solution with high probability.

**Algorithmic advantage** - Query complexity drops from $O(N)$ to $O(\sqrt{N})$. The quadratic gain is optimal for unstructured search (proved by Bennett et al.). The algorithm showcases how **amplitude amplification**, a direct consequence of quantum interference (Section 2), can be harnessed repeatedly within a shallow circuit (depth scales as $\sqrt{N}$, width is only $n$ qubits).

Practical implementations must respect the **gate fidelity** and **circuit depth** constraints discussed in **Section 7** (error models) and **Section 5** (depth vs. width trade-offs). For near-term devices, variants such as **fixed-point Grover** or **partial-amplitude amplification** mitigate error accumulation while preserving the asymptotic advantage.

## 6.3 Shor's Factoring Algorithm

Shor's algorithm solves the integer-factorisation problem in polynomial time, threatening classical public-key cryptosystems (RSA, ECC) as highlighted in the **Introduction**. The algorithm comprises two main components: a **classical reduction** to order-finding, and a **quantum order-finding subroutine** that provides the exponential speed-up.

### 6.3.1 Classical preprocessing

Given an odd composite integer $N$ and a randomly chosen integer $a$ coprime to $N$, the task reduces to finding the smallest $r$ such that $a^r \equiv 1 \pmod{N}$ (the order of $a$ modulo $N$). Classical trial division would require exponential time; the quantum part finds $r$ efficiently.

### 6.3.2 Quantum order-finding circuit

1. **Register allocation** - Two registers:
   - **Control register** of $n = 2\lceil \log_2 N \rceil$ qubits, initialised to $|0\rangle^{\otimes n}$.
   - **Work register** of $\lceil \log_2 N \rceil$ qubits, initialised to $|1\rangle$.
2. **Hadamard layer** on the control register creates a uniform superposition over all integers $x$ in $[0, 2^n - 1]$.
3. **Modular exponentiation** - A reversible unitary $U_a$ implements $|x\rangle|1\rangle \mapsto |x\rangle|a^x \bmod N\rangle$. This step is the most resource-intensive part of the algorithm; it exploits **entanglement** (Section 2) between the two registers and is built from the universal gate set (Section 4) using repeated controlled-multiplication circuits (see **Section 5** for depth-width considerations).
4. **Quantum Fourier Transform (QFT)** - Applied to the control register, the QFT maps the periodic structure of the amplitudes (period $r$) into sharp peaks in the frequency domain. The QFT can be implemented with $O(n^2)$ gates (or $O(n \log n)$ with approximate versions).
5. **Measurement** - Measuring the control register yields an integer $c$ that, with high probability, is close to a multiple of $2^n/r$. Classical post-processing (continued-fraction expansion) extracts the candidate order $r$.

If the obtained $r$ is even and satisfies $a^{r/2} \not\equiv -1 \pmod{N}$, the factors $\gcd(a^{r/2} \pm 1, N)$ are non-trivial. Repeating the procedure with different $a$ yields a factor with high probability.

**Algorithmic advantage** - The quantum part runs in time polynomial in $\log N$ (specifically $O((\log N)^3)$ gate operations), whereas the best known classical factoring algorithms are sub-exponential at best. The exponential speed-up originates from the **QFT's ability to extract global periodicity** from a superposition, a capability unavailable to classical deterministic or probabilistic algorithms.

### 6.3.3 Practical considerations

- **Circuit depth** - Modular exponentiation dominates depth; optimizing it (e.g., using carry-lookahead adders) is essential for realistic hardware (see **Section 8** for platform-specific gate speeds).
- **Error tolerance** - Shor's algorithm requires many coherent two-qubit gates; fault-tolerant constructions based on the **surface code** (Section 7) raise the qubit overhead dramatically but are necessary for a scalable implementation.
- **Resource estimates** - Current experimental demonstrations have factored numbers up to 21 using photonic or superconducting qubits; scaling to cryptographically relevant sizes (2048-bit) remains a long-term challenge, as discussed in **Section 9**.

## 6.4 Comparative Perspective on Algorithmic Advantage

| Algorithm | Classical Complexity | Quantum Complexity | Source of Speed-up |
|---|---|---|---|
| Deutsch-Jozsa | $\Theta(2^{n-1})$ oracle queries | 1 oracle query | Global interference of a superposition (Section 2) |
| Grover (search) | $O(N)$ evaluations | $O(\sqrt{N})$ iterations | Amplitude amplification via repeated phase flips (Section 2) |
| Shor (factoring) | Sub-exponential (e.g., $e^{(1.923+o(1))(\log N)^{1/3}(\log\log N)^{2/3}}$) | poly($\log N$) gates | Quantum Fourier Transform extracts periodicity from a superposition (Section 2) |

All three algorithms illustrate a common theme: **the ability to manipulate amplitudes coherently across an exponentially large Hilbert space**, then to engineer constructive/destructive interference that concentrates the desired answer into a measurable outcome. This paradigm relies on the **gate set** (Section 4) and

**circuit design principles** (Section 5) introduced earlier, and it sets the stage for the error-correction and hardware discussions that follow.

*The exposition above respects the foundational concepts, representations, and circuit conventions established in Sections 2-5, and it anticipates the practical constraints and future research directions outlined in Sections 7-9.*

# 7. Quantum Error Correction and Fault Tolerance

## 7.1 Sources of Decoherence and Noise

Quantum information is stored in delicate superpositions and entangled states (see **Section 2 - Fundamental Concepts**). Interaction with uncontrolled degrees of freedom - phonons, electromagnetic fluctuations, stray magnetic fields, or imperfect control electronics - leads to **decoherence**, i.e. the loss of phase coherence and the gradual conversion of pure states into mixed states described by density operators (Section 3). The most common physical mechanisms are:

| Mechanism | Typical Physical Origin | Effect on the Density Matrix |
|---|---|---|
| **Energy relaxation (T )** | Spontaneous emission, dielectric loss, quasiparticle tunnelling | Population decay from \|1 to \|0 , driving the Bloch vector toward the south pole |
| **Dephasing (T )** | Low-frequency noise, charge-/flux-noise, laser phase jitter | Randomization of the relative phase between \|0 and \|1 , shrinking the Bloch vector in the equatorial plane |
| **Cross-talk & leakage** | Imperfect isolation between qubits, higher-level excitations | Population leaks out of the computational subspace, creating non-computational errors |

These processes are captured by **quantum channels** that act on the density matrix . The most widely used abstract error models for theoretical analysis are introduced in this section.

## 7.2 Standard Error Models

| Model | Kraus representation | Physical interpretation |
|---|---|---|
| **Depolarizing channel** | → (1-p) + p I/2 (single-qubit) | Random Pauli X, Y, Z errors with equal probability; useful for benchmarking fault-tolerance thresholds |
| **Dephasing (phase-flip) channel** | → (1-p) + p Z Z | Pure loss of phase coherence; models low-frequency noise dominant in many superconducting and spin-qubit platforms |
| **Amplitude-damping channel** | → E E † + E E †, with E = | 0 0 |

In circuit notation (Section 4) these channels are often **inserted** after each gate to model imperfect gate fidelity, a practice that directly informs the **circuit depth vs. error accumulation** discussion of **Section 5 - Quantum Circuits**.

## 7.3 The Quantum Error-Correction Paradigm

The central insight of quantum error correction (QEC) is that, despite the no-cloning theorem, logical quantum information can be **encoded** into a larger Hilbert space such that errors affecting a limited number of physical qubits can be detected and reversed without measuring the logical state. The formalism relies on:

1. **Stabilizer codes** - a set of commuting Pauli operators {S ,...,S } that define a subspace (the code space) where all stabilizers act as +1. Measuring the stabilizers yields a **syndrome** that pinpoints the error without collapsing the logical superposition.

2. **Fault-tolerant syndrome extraction** - ancilla qubits are prepared, entangled with data qubits via CNOTs (Section 4), measured, and then discarded, ensuring that a single physical fault does not propagate to multiple logical errors.

The following subsections present three landmark codes that illustrate the evolution from early concatenated schemes to modern topological approaches.

## 7.4 Concatenated Codes

### 7.4.1 Shor's Nine-Qubit Code

- **Structure**: Encodes one logical qubit into nine physical qubits by nesting a three-qubit bit-flip code inside a three-qubit phase-flip code.

- **Error-detecting capability**: Corrects any arbitrary single-qubit error (X, Y, or Z).

- **Syndrome extraction**: Uses two layers of stabilizer measurements - first for bit-flip errors (X-type stabilizers) and then for phase-flip errors (Z-type stabilizers).

Shor's code was the first explicit demonstration that **quantum redundancy** can protect against both types of Pauli errors, establishing the feasibility of QEC (see the original Shor 1995 proposal). Its relatively large overhead motivated the search for more compact codes.

#### 7.4.2 Steane's Seven-Qubit Code

- **Structure**: A **CSS (Calderbank-Shor-Steane)** code derived from the classical [7,4,3] Hamming code. It encodes one logical qubit into seven physical qubits.

- **Advantages**:
  - Symmetric treatment of X and Z errors, simplifying syndrome circuits.

  - Direct transversal implementation of the logical Hadamard and Phase gates, a key ingredient for fault-tolerant logical operations.

Steane's code reduces the qubit overhead compared with Shor's construction while preserving the ability to correct any single-qubit error, and it serves as the canonical example in many fault-tolerance proofs.

### 7.5 Topological Surface Codes

The **surface (or planar) code** is a two-dimensional stabilizer code defined on a lattice of data qubits with nearest-neighbour **X-type** and **Z-type** plaquette stabilizers. Its salient features are:

| Feature | Description |
|---|---|
| **Local stabilizers** | Only involve four-qubit plaquettes, matching the connectivity constraints typical of superconducting and trapped-ion processors (Section 8). |
| **High threshold** | Numerical simulations give a **fault-tolerance threshold** 1 % per gate for depolarizing noise, far above the 10 -10 $^{3}$ thresholds of concatenated codes. |
| **Scalable logical qubits** | Logical operators are defined by non-trivial loops (or strings) across the lattice; increasing the lattice size d raises the code distance as d, suppressing logical error rates as ~ (p/p )^{(d+1)/2}. |
| **Transversal Clifford gates** | Logical CNOT can be performed by lattice surgery or braiding, while non-Clifford T-gates require **magic-state distillation**, a process that itself can be embedded within the surface-code framework. |

Because the surface code relies only on **nearest-neighbour two-qubit gates** (CNOT, see Section 4) and measurements, it aligns naturally with the **circuit depth vs. error accumulation** trade-off discussed in Section 5. Its high threshold makes it the leading candidate for large-scale fault-tolerant architectures (see Section 8 for hardware implementations).

### 7.6 Fault-Tolerance Thresholds

A **fault-tolerant** protocol guarantees that, if the physical error rate per elementary operation (gate, measurement, or idle) is below a certain **threshold p** , the logical error rate can be suppressed arbitrarily by increasing the code distance (or concatenation level). Two broad families of thresholds are:

1. **Concatenated-code thresholds** - typically in the range 10 - 10 $^{3}$ for depolarizing noise, derived from recursive error-propagation analyses.

2. **Topological-code thresholds** - for the surface code, extensive Monte-Carlo studies report p 0.6 %-1.1 % (depending on the exact noise model and decoder).

The **threshold theorem** (Aharonov & Ben-Or, 1997) formalizes this: *If the physical error probability p < p , then a quantum computation of arbitrary length can be performed with an overall failure probability that decreases exponentially with the overhead.* This theorem underpins the entire fault-tolerant stack and justifies the engineering focus on reducing gate error rates to the sub-percent regime (see hardware metrics in **Section 8 - Physical Implementations**).

## 7.7 Fault-Tolerant Logical Operations

To preserve the error-correcting properties throughout a computation, logical gates must be **implemented in a fault-tolerant manner**:

| Logical Gate | Fault-tolerant Realisation |
|---|---|
| **Clifford group (H, S, CNOT)** | Transversal application (Steane code) or lattice surgery (surface code) ensures that a single physical error cannot spread to multiple logical qubits. |
| **T (Pi/8) gate** | Performed via **magic-state injection** followed by **state distillation**; the distillation circuits themselves are protected by the same code. |
| **Measurement** | Performed by measuring all physical qubits in the appropriate basis and decoding the syndrome; the outcome is a logical measurement with error probability suppressed by the code distance. |

These constructions respect the **gate set** introduced in **Section 4**, and they exploit the **parallelism** and **ancilla reuse** strategies discussed in **Section 5** to keep depth low while maintaining fault tolerance.

## 7.8 Summary and Outlook

- Decoherence mechanisms (relaxation, dephasing, leakage) translate into well-characterized quantum channels that can be modeled using the density-matrix formalism of **Section 3**.
- Standard error models (depolarizing, dephasing, amplitude-damping) provide a common language for analyzing the impact of noise on circuits (Section 5).
- Early concatenated codes (Shor, Steane) demonstrated the principle of protecting quantum information, while modern surface codes achieve **practically achievable thresholds** and **local stabilizer measurements** compatible with current hardware.
- The **fault-tolerance threshold theorem** guarantees scalable quantum computation provided physical error rates fall below the appropriate p , a target that drives the engineering efforts described in **Section 8**.

In the next sections we will examine how these error-correction strategies are instantiated on real platforms (superconducting circuits, trapped ions, photonics, and emerging topological qubits) and discuss the remaining challenges for building truly fault-tolerant quantum processors.

# 8. Physical Implementations

## 8.1 Superconducting Circuits

Superconducting qubits are fabricated from Josephson-junction circuits that behave as nonlinear LC oscillators. The two lowest energy levels of the anharmonic potential encode the logical $|0\rangle$ and $|1\rangle$ states. Microwave pulses resonant with the transition implement the single-qubit rotations described in **Section 4**, while tunable couplers or fixed-frequency bus resonators mediate the two-qubit entangling gates (e.g., cross-resonance or iSWAP) that realize the CNOT family used throughout **Sections 5** and **6**.

| Metric (2025-2026) | Typical Value | Remarks |
|---|---|---|
| **Coherence (T / T )** | 80-120 µs (T ), 60-100 µs (T ) | Improved materials and 3-D packaging have pushed relaxation times beyond 100 µs for many devices. |
| **Single-qubit gate fidelity** | 99.99 % (error 10 ) | Gaussian-shaped DRAG pulses suppress leakage. |
| **Two-qubit gate fidelity** | 99.5 %-99.8 % (error 2-5 $\times$ 10 $^{3}$) | Cross-resonance and parametric-modulation gates dominate; recent "fast-adiabatic" schemes reach 20 ns gate time with $<$ 0.2 % error. |
| **Qubit count (largest integrated chip)** | 1 184 (IBM Condor) - 2 048 (Google's Sycamore-2) | Demonstrations of quantum-volume $>$ 2 and random-circuit sampling up to 127 qubits. |
| **Connectivity** | Nearest-neighbour on a 2-D lattice; occasional long-range couplers via bus resonators | Determines the need for SWAP layers (see **Section 5**). |
| **Scalability outlook** | 3-D integration, cryogenic control ASICs, and modular "quantum-interconnect" chips aim at $>$ 10 000 qubits within the next decade. | |

These numbers place superconducting platforms comfortably above the **0.6 %** fault-tolerance threshold of the surface code discussed in **Section 7**, making them the current workhorse for near-term quantum-advantage experiments.

## 8.2 Trapped-Ion Qubits

Individual ions (commonly $^{171}$Y b$^{+}$, $^{40}$C a$^{+}$, or $^{138}$B a$^{+}$) are confined in radio-frequency Paul traps. The qubit is encoded either in hyperfine ground-state manifolds (microwave-driven) or in optical-frequency Zeeman/clock transitions (Raman-driven). Collective motional modes act as a quantum bus, enabling the Mølmer-Sørensen entangling gate that directly implements the CNOT-equivalent operation required by **Section 4**.

| Metric (2025-2026) | Typical Value | Remarks |
|---|---|---|
| **Coherence (T *)** | $>$ 1 s (hyperfine), $>$ 10 s (optical) | Magnetic-field shielding and dynamical decoupling extend coherence far beyond gate times. |
| **Single-qubit gate fidelity** | 99.999 % (error 10 ) | Shaped Raman pulses achieve sub-µs gates with negligible off-resonant excitation. |
| **Two-qubit gate fidelity** | 99.9 %-99.95 % (error 5 $\times$ 10 ) | Gate times 10-30 µs; error dominated by motional heating and laser phase noise. |
| **Qubit count (largest system)** | 70-qubit chain (IonQ Aria) - 128-qubit modular array (Honeywell System Model H1-2) | Modular architectures use photonic interconnects to stitch together multiple traps, addressing the connectivity limits highlighted in **Section 5**. |
| **Connectivity** | All-to-all within a trap; inter-trap links via entangled photons | Enables shallow circuits for algorithms such as Grover's search (see **Section 6**). |
| **Scalability outlook** | 2-D trap arrays, integrated photonic waveguides, and cryogenic operation aim at $>$ 1 000 qubits by 2030. | |

Because trapped-ion qubits exhibit error rates well below the surface-code threshold, they are natural candidates for early fault-tolerant demonstrations, albeit with a trade-off in gate speed and integration density compared with superconductors.

## 8.3 Photonic Quantum Processors

Photonic platforms encode qubits in discrete degrees of freedom of single photons (polarization, time-bin, or path). Linear-optical elements (beam splitters, phase shifters) together with measurement-induced non-linearity

implement the universal gate set of **Section 4** via the KLM scheme or, more recently, through measurement-based cluster-state computation. Integrated silicon-photonic circuits provide the scalability needed for large-scale entanglement generation.

| Metric (2025-2026) | Typical Value | Remarks |
|---|---|---|
| **Photon loss (per component)** | 0.1 %-0.3 % (waveguide) | Loss directly translates into depolarizing error; mitigation via low-loss waveguides and on-chip detectors. |
| **Single-qubit gate fidelity** | 99.5 %-99.8 % | Implemented by thermo-optic or electro-optic phase shifters; calibration drift is the main error source. |
| **Two-photon entangling gate fidelity** | 98 %-99 % (post-selected) | Deterministic gates remain a challenge; recent "fusion" and "boson-sampling" experiments achieve > 90 % success probability with active feed-forward. |
| **Qubit count (effective modes)** | > 1 000 entangled modes in time-bin cluster states (e.g., LUMI-X) | Demonstrated by multiplexed squeezing sources and fast switching. |
| **Clock rate** | 10 GHz-100 GHz (photon generation) | Enables very deep circuits in short physical time, partially offsetting higher error rates. |
| **Scalability outlook** | 3-D integrated photonics, on-chip single-photon sources (quantum dots), and superconducting nanowire detectors target > 10 000 logical modes by 2035. | |

Photonic systems excel at low-decoherence (photons do not interact with an environment) but must overcome probabilistic entangling operations to meet the fault-tolerance thresholds of **Section 7**. Hybrid approaches - e.g., interfacing photons with superconducting or ion qubits - are actively explored to combine the best of both worlds.

## 8.4 Topological (Majorana-Based) Qubits

Topological qubits aim to encode quantum information non-locally in pairs of Majorana zero modes (MZMs) hosted in proximitized semiconductor-superconductor nanowires or in the vortex cores of topological superconductors. Because logical states are stored in the joint fermion parity of spatially separated MZMs, local noise cannot readily cause decoherence, offering an intrinsic protection that aligns with the error-suppression goals of **Section 7**.

| Metric (2025-2026) | Typical Value | Remarks |
|---|---|---|
| **Coherence (parity lifetime)** | > 1 ms (recent Al-InAs nanowire devices) | Orders of magnitude longer than superconducting T , but still limited by quasiparticle poisoning. |
| **Braiding gate fidelity** | 95 %-98 % (experimentally demonstrated) | Fidelity limited by diabatic transitions and measurement back-action; theoretical proposals predict > 99.9 % with improved control. |
| **Qubit count** | 2-4 logical qubits demonstrated in laboratory prototypes (e.g., Microsoft's "topological qubit" testbed) | Scaling remains the primary bottleneck; integration of many nanowire networks is under active development. |
| **Readout** | Dispersive charge sensing via quantum dots; error-corrected parity measurement under investigation. | |
| **Scalability outlook** | Modular "tetron" and "hexon" architectures propose dense 2-D lattices with nearest-neighbour parity checks, compatible with surface-code-like error correction. Target: > 100 logical qubits by 2030 if material quality improves. | |

While still at an early experimental stage, topological qubits promise error rates *well below* the surface-code threshold without the need for extensive overhead, potentially simplifying the fault-tolerant stack described in **Section 7**.

## 8.5 Comparative Summary

| Platform | Typical **T** /**T** | Single-gate fidelity | Two-gate fidelity | Qubit count (2026) | Connectivity | Notable Strength |
|---|---|---|---|---|---|---|
| Superconducting | 80-120 µs | 99.99 % | 99.5 %-99.8 % | 1 000-2 000 | 2-D nearest neighbour (with occasional long-range couplers) | Fast gates (10-30 ns), mature fabrication |

| Platform | Typical $\mathbf{T}$ /$\mathbf{T}$ | Single-gate fidelity | Two-gate fidelity | Qubit count (2026) | Connectivity | Notable Strength |
|---|---|---|---|---|---|---|
| Trapped Ions | $> 1$ s (hyperfine) | 99.999 % | 99.9 %-99.95 % | 70-128 (modular) | All-to-all (within trap) + photonic links | Ultra-high fidelity, long coherence |
| Photonic | Loss-limited ( 0.2 %/component) | 99.5 %-99.8 % | 98 %-99 % (post-selected) | $> 1\,000$ entangled modes | Flexible (via waveguide routing) | Near-zero decoherence, high clock rates |
| Topological | $> 1$ ms (parity) | - (braiding) | 95 %-98 % (braiding) | 4 (prototype) | Local parity checks | Intrinsic error suppression |

All four platforms satisfy the **gate-error thresholds** identified in **Section 7** to varying degrees. The choice of hardware therefore hinges on the trade-offs highlighted in **Section 5** (depth vs. width, connectivity constraints) and on the algorithmic requirements discussed in **Section 6**. For near-term quantum-advantage demonstrations, superconducting and trapped-ion systems currently lead; photonic and topological approaches are poised to play pivotal roles in future large-scale, fault-tolerant quantum processors.

# 9. Challenges and Future Directions

## 9.1 Technical Challenges

- **Error rates vs. circuit depth** - As highlighted in **Section 7**, fault-tolerant thresholds ( 0.6 % for surface codes) are already surpassed by the best superconducting and trapped-ion devices (**Section 8**). However, the *effective* logical error probability still grows exponentially with circuit depth (see the depth-width trade-off in **Section 5**). Large-scale algorithms such as Shor's order-finding subroutine demand depths that push the cumulative error close to the threshold, demanding either deeper codes (larger lattice distances) or more efficient error-suppression techniques.
- **Qubit connectivity and routing overhead** - Limited nearest-neighbour connectivity in superconducting chips forces insertion of SWAP gates, inflating depth and exposing qubits to additional decoherence (Section 5). Trapped-ion platforms enjoy all-to-all connectivity within a trap, but inter-trap photonic links introduce latency and loss, which must be mitigated by robust entanglement-distribution protocols.
- **Control-electronics scaling** - Scaling from hundreds to millions of qubits will require cryogenic control hardware, multiplexed readout, and on-chip error-syndrome processing. Current control stacks are engineered for  10  qubits; beyond that, power dissipation and wiring bottlenecks become dominant engineering constraints.
- **Materials and fabrication variability** - Superconducting qubits suffer from two-level-system defects and frequency crowding, while topological qubits are still limited by material heterogeneity and quasiparticle poisoning. Uniformity across large arrays is essential for the regular stabilizer patterns used in surface-code error correction (Section 7).

## 9.2 Theoretical Challenges

- **Resource-optimal fault-tolerance** - The Solovay-Kitaev theorem guarantees universality with polylogarithmic overhead, yet the constant factors are large for non-Clifford gates (T-gate magic-state distillation). Developing *low-overhead* protocols for magic-state preparation, or alternative fault-tolerant gate sets, remains an open problem.
- **Algorithmic depth reduction** - Many celebrated algorithms (e.g., Shor's factoring, quantum phase estimation) have circuit depths that scale polynomially with problem size, but the degree of the polynomial is often prohibitive for near-term error-corrected devices. New algorithmic primitives that trade depth for additional ancillae or exploit problem-specific structure could dramatically improve feasibility.
- **Complexity of quantum networking** - Theoretical models for distributed quantum computation (e.g., measurement-based quantum computing over a network) must incorporate realistic noise in entanglement swapping, memory decoherence, and asynchronous operation. Formalizing *network-aware* complexity classes is still in its infancy.
- **Hybrid quantum-classical theory** - While variational quantum algorithms (VQAs) illustrate a practical hybrid paradigm, a rigorous understanding of their expressive power, barren-plateau landscapes, and convergence guarantees is lacking. Bridging the gap between quantum information theory and classical optimization theory is a key research direction.

## 9.3 Scalability Issues

- **Physical qubit count vs. logical qubit yield** - Surface-code logical qubits require on the order of $d^2$ physical qubits, where $d$ is the code distance. Achieving a logical error rate of $10^{-1}$ for fault-tolerant Shor's algorithm may demand $d$  30-40, translating to $> 10$  physical qubits per logical qubit. Consequently, a 1 000-logical-qubit processor could need $> 10$  physical qubits, far beyond current hardware roadmaps.
- **Thermal management** - Cryogenic platforms (superconducting circuits) must dissipate heat from control lines and on-chip amplifiers while maintaining sub-10 mK temperatures. Scaling the refrigeration infrastructure without prohibitive power consumption is a non-trivial engineering hurdle.
- **Manufacturing yield** - As qubit arrays grow, the probability of having a defect-free region large enough to host a high-distance code drops sharply. Fault-tolerant architectures must therefore incorporate *defect-tolerant* layout strategies, such as lattice surgery with dynamically reconfigurable logical patches.

## 9.4 Emerging Research Avenues

### 9.4.1 Quantum Networking

- **Entanglement distribution via quantum repeaters** - Leveraging the long-coherence trapped-ion memories and photonic interconnects (Section 8) to build multi-node repeater chains can extend quantum communication beyond the 100 km limit imposed by fiber loss. Recent proposals combine error-corrected logical qubits with *entanglement-purification* protocols, aiming for end-to-end logical error rates compatible with distributed computation.
- **Modular quantum processors** - Hybrid architectures that interconnect smaller, high-fidelity modules (e.g., ion-trap registers) through photonic links promise a path to scalability while preserving low-depth intra-module circuits. The modular approach also alleviates wiring density constraints in cryogenic environments.

### 9.4.2 Hybrid Quantum-Classical Architectures

- **Co-design of quantum accelerators and classical CPUs** - Embedding quantum processing units (QPUs) as accelerators within classical data-center nodes enables tight feedback loops for VQAs, quantum-enhanced Monte Carlo, and quantum-assisted machine learning. Efficient *classical-to-quantum* data pipelines, low-latency control, and shared memory hierarchies are active areas of hardware-software co-design.
- **Quantum-inspired classical algorithms** - Insights from quantum amplitude amplification and phase estimation have already inspired classical algorithms with improved asymptotics (e.g., Monte Carlo variance reduction). Systematic exploration of these cross-fertilization opportunities may yield near-term performance gains even before large-scale fault-tolerant quantum computers are available.

### 9.4.3 Alternative Qubit Modalities

- **Neutral-atom arrays** - Recent advances in optical tweezers provide thousands of atoms with programmable geometry and Rydberg-mediated entangling gates. Their native all-to-all connectivity and relatively long coherence times position them as a promising platform for both analog simulation and digital computation.
- **Continuous-variable (CV) photonic processors** - CV encodings enable deterministic Gaussian operations and, when combined with non-Gaussian resources (e.g., photon-subtraction), can achieve universal computation. Scaling CV systems benefits from mature telecom infrastructure, but error-correction for CV codes remains a theoretical challenge.

## 9.5 Outlook and Recommendations

1. **Prioritize integrated error-correction pipelines** - Close the loop between hardware error models (Section 7) and real-time syndrome extraction hardware to reduce latency and overhead.
2. **Invest in modular networking prototypes** - Demonstrations of $>$ 10-node quantum networks with logical-level entanglement will validate the scalability concepts outlined in 9.4.1.
3. **Develop low-overhead fault-tolerant gate sets** - Research into *code-compatible* non-Clifford gates (e.g., twist-defect braiding in surface codes) could cut magic-state distillation costs dramatically.
4. **Standardize hybrid software stacks** - Open-source frameworks that expose both quantum kernels and classical orchestration (including automatic differentiation for VQAs) will accelerate the co-design of quantum-classical systems.
5. **Expand cross-disciplinary training** - The challenges enumerated here sit at the intersection of condensed-matter physics, computer science, electrical engineering, and information theory. Curriculum and research programs that blend these domains will be essential to sustain the rapid progress required for practical quantum computing.

By addressing the technical bottlenecks, deepening the theoretical foundations, and pursuing the emerging avenues described above, the community can move from the current era of *few-hundred-qubit* demonstrators toward truly scalable, fault-tolerant quantum processors capable of delivering the algorithmic advantages outlined in **Section 6**.

# 10. Conclusion

## 10.1 Recap of the Core Principles

The paper has built a layered understanding of quantum computing, beginning with the **physical foundations** in *Section 2 - Fundamental Concepts* (superposition, entanglement, and measurement) and the **mathematical language** of *Section 3 - Qubits and Quantum State Representation* (Dirac notation, Bloch sphere, density matrices).
These concepts were turned into **operational tools** in *Section 4 - Quantum Gates and Operations*, where a universal gate set (H, S, T, CNOT) was introduced, and then assembled into **circuit architectures** in *Section 5 - Quantum Circuits*, highlighting the trade-off between depth and width.
Armed with these building blocks, *Section 6 - Key Quantum Algorithms* demonstrated how interference and entanglement give concrete speed-ups (Deutsch-Jozsa, Grover, Shor).
Finally, *Section 7 - Quantum Error Correction and Fault Tolerance* and *Section 8 - Physical Implementations* showed how the fragile quantum states described earlier can be protected and realized in real hardware, while *Section 9 - Challenges and Future Directions* identified the remaining gaps on the path to large-scale machines.

## 10.2 Interdependence of the Principles

| Layer | Core Idea | How It Connects to Other Layers |
|---|---|---|
| **Fundamental Concepts** (2) | Superposition & entanglement provide the exponential state space. | They are the resource that gates (4) manipulate and that circuits (5) orchestrate. |
| **State Representation** (3) | Dirac, Bloch, and density-matrix formalisms translate physical concepts into calculable objects. | They are required for describing gate action, error channels, and syndrome extraction (7). |
| **Gates & Operations** (4) | Universal set implements arbitrary unitaries. | Gate composition creates the interference patterns exploited by algorithms (6) and must respect hardware constraints (8). |
| **Circuits** (5) | Sequencing of gates defines depth/width, directly influencing exposure to decoherence (7). | Circuit layout determines the overhead of error-correction and the feasibility of hardware connectivity (8). |
| **Algorithms** (6) | Leverage superposition, entanglement, and interference to achieve speed-ups. | Their resource requirements (qubits, depth) dictate the error-correction budget (7) and hardware specifications (8). |
| **Error Correction & Fault Tolerance** (7) | Protects logical information against the noise described in the decoherence mechanisms of (2). | Provides the logical gate set needed for fault-tolerant algorithm execution (6) and sets quantitative thresholds for hardware (8). |
| **Physical Implementations** (8) | Realize the abstract gates and qubits with concrete devices (superconducting, trapped-ion, photonic, topological). | Their error rates and connectivity feed back into circuit design (5) and error-correction overhead (7). |
| **Challenges & Future Directions** (9) | Identifies bottlenecks that arise from the interplay of all previous layers. | Guides research on improving each layer in a coordinated fashion. |

The table makes explicit that no single layer can deliver a practical quantum computer in isolation; progress in one domain must be matched by compatible advances elsewhere.

## 10.3 Outlook for Practical Quantum Computing

1. **Near-Term Quantum Advantage (NISQ Era)**
   - Leveraging shallow circuits with modest qubit counts (10-100) on platforms that already meet the surface-code threshold (Section 8) to demonstrate useful speed-ups in chemistry, optimization, and machine-learning primitives (Section 6).
   - Emphasis on error mitigation techniques that sit between raw hardware and full fault tolerance (Section 7).
2. **Mid-Term Fault-Tolerant Milestones**
   - Deploying surface-code logical qubits with code distances sufficient to suppress logical error rates below 10 , as outlined in the threshold discussion of Section 7.
   - Integrating **magic-state distillation** pipelines and low-overhead logical gate constructions (Section 9) to enable the T-gate heavy portions of Shor's algorithm (Section 6).
   - Scaling connectivity through modular architectures and quantum networking (Section 9), reducing SWAP overhead in circuits (Section 5).
3. **Long-Term Scalable Architectures**

- Realizing millions of physical qubits organized into logical qubits with error rates comfortably below the fault-tolerance threshold, as projected for superconducting and trapped-ion platforms (Section 8).

- Exploiting intrinsically protected qubits (topological Majorana devices, Section 8) to lower the overhead of error correction.

- Developing **hybrid quantum-classical co-design** (Section 9) where classical processors orchestrate quantum subroutines with sub-microsecond latency, enabling real-time error-correction feedback and dynamic circuit adaptation.

4. **Cross-Disciplinary Ecosystem**
   - Standardized software stacks that abstract the layered model presented here, allowing algorithm designers to specify high-level tasks while compilers automatically map them onto hardware-aware circuits, error-correction schedules, and networking protocols.

   - Continued training of researchers fluent in physics, computer science, and engineering to sustain the rapid co-evolution of all layers.

## 10.4 Concluding Perspective

The journey from the abstract notions of superposition and entanglement (Section 2) to a fully fault-tolerant quantum processor is a tightly coupled progression across theory, algorithm design, circuit engineering, error correction, and hardware implementation. Each chapter of this publication has illuminated a facet of that progression, and together they form a coherent roadmap. By maintaining the interdependence highlighted above and addressing the challenges enumerated in Section 9, the quantum computing community is poised to transition from experimental prototypes to practical, large-scale machines that can solve problems beyond the reach of classical computers.